1991 ASCE Geotechnical Engineering Congress
Boulder, Colorado, June 9-12, 1991

WAVE EQUATION MODELLING OF THE SPT

Alex Sy[1], M.ASCE and R.G. Campanella[2], M.ASCE

ABSTRACT: The stress wave propagation in the Standard Penetration Test (SPT) is described in this paper. It is shown that the SPT is a complex dynamic system and that both force and motion measurements are needed to fully characterize the wave propagation in the SPT drill rod and sampler system. Field measurements of force and acceleration time histories in the SPT drill rods are presented. It is shown that a study of the force and velocity traces can give considerable insight into the dynamics of the SPT. The results of wave equation analyses of the SPT are compared to the field stress wave measurements.

INTRODUCTION

The Standard Penetration Test (SPT) is the most widely used in-situ test in North America and has been correlated to many geotechnical design parameters. Despite continued efforts to standardize the SPT equipment and test procedure, there are still problems associated with its repeatability and reliability. Numerous studies in recent years have shown that there are many factors influencing the SPT results, but the most significant factor affecting the N-value is the amount of hammer energy delivered into the drill rods. Several investigators have measured the hammer energy in various SPT systems and found considerable variabilities (Smith, 1977; Kovacs and Salomone, 1982; Robertson et al. 1983; Riggs et al. 1984).

To understand the SPT energy dynamics and sampling process, several researchers have attempted to analyze the SPT by the one-dimensional wave equation model commonly used for pile driving analysis. Early studies by Adam (1971) and McLean et al. (1975) on wave equation analysis of the SPT were concentrated mainly on investigating the effects on N-value of factors such as height of hammer drop, anvil size, rod type and length, slack at rod joints and soil resistance. It was found that the height of drop, or hammer energy, and soil resistance were the major factors influencing N-values. However, no experimental or field verification was presented.

---

1 - Ph.D. Student, Dept. of Civil Engin., Univ. of British Columbia, Vancouver, B.C., Canada, V6T 1W5.
2 - Professor, Dept. of Civil Engin., Univ. of British Columbia, Vancouver, B.C., Canada, V6T 1W5.

Schmertmann and his co-workers at the University of Florida conducted a comprehensive theoretical and experimental study of the energy dynamics of the SPT (Schmertmann, 1978; Schmertmann and Palacios, 1979; Palacios, 1977). They traced the stress wave theoretically from impact through the drill rods to the sampler tip and returning back to the top of the drill string. In their field experiment, they incorporated load cells near the top and bottom of the drill rods to measure the force-time histories of the stress waves. The force data were used to calculate energy transfer in the rods and the energy loss in the sampling process. They showed field data to confirm that N-value varies inversely with energy delivered into the drill rods.

The University of Florida group also conducted wave equation studies to simulate the dynamics of the SPT (Gallet, 1976; Hanskat, 1978). They were able to obtain reasonable match of the computed results to the measured force-time data in the drill rods, transfer energy in the rods and sampler penetration. Their wave equation studies indicated negligible effect on the N-value (hence transferred energy) of the type of rods (A or N type), type of hammers (donut or safety), rod whipping, damping losses in rods and tightness of rod joints. Since the driving of the SPT is analogous to the driving of a pile, they suggested the use of the SPT and wave equation modelling to estimate the soil damping coefficients for wave equation analysis of piles.

Bosscher and Showers (1987) used a wave equation program to model the SPT to study the effect of soil type on impact energy in the drill rods. Wave equation modelling of the SPT has also recently been used to predict bearing capacity of soil layers (Ellstein, 1988).

Clearly, the wave equation model has the potential for analyzing the dynamics of the SPT. The results of the wave equation analysis, however, should be checked against field measurements of stress wave propagation in the drill rods. It will be shown in this paper that both force and motion measurements in the drill rods are needed to fully characterize the stress waves in the SPT system. Successful theoretical modelling and verification of the SPT will give more insight into the mechanics of impact wave propagation in the SPT system and allow more confident use of the SPT for geotechnical design.

This paper presents the results of a wave equation study of the SPT dynamics using the GRLWEAP program (Goble Rausche Likins and Associates, Inc., 1990). The calculated force and velocity time histories are compared to force and velocity measurements obtained in the field.

STRESS WAVE PROPAGATION IN THE SPT

On hammer impact in the SPT, compression waves are generated which travel simultaneously with the same velocity down the drill rods and up the hammer. The speed of wave propagation is a constant, being about 16,800 ft/sec (5100 m/s) in steel. For a compression pulse (positive force), the particle motion is in the same direction as the direction of wave propagation, whereas for a tension pulse (negative force), the particle motion is in the opposite direction to wave propagation. The stress waves reflect with opposite sign at the ends of the rods or hammer, i.e. compression to tension to compression, etc.

Because the hammer is usually much shorter than the rod and sampler system, more wave returns or cycles occur in the hammer than in the rods at any given time after impact. Each time the wave in the hammer returns to the hammer-anvil contact, some more energy is transferred to the rods, the amount decreasing with each wave cycle.

Figure 1 shows an idealized force-time waveform recorded near the top of the drill rods due to a SPT hammer impact. The impact pulse has a short rise time to the peak force, followed by a longer fall time during which the force decays gradually with each wave travel cycle in the hammer. Point (2) in Figure 1 marks the arrival of the tensile wave reflection from the sampler and is commonly referred to as the tension cutoff time. Note that the time interval from the point of impact represented by the first force peak to the tension cutoff point is 2L/c, in which L is the length of the SPT rod and sampler system below the load cell and c is the speed of wave propagation in the drill rods. The 2L/c is the time it takes for the impact wave to travel from the load cell near the top of the drill rods to the sampler bottom and return to the load cell location. After hammer impact, the hammer and rods remain in contact only until the tension cutoff occurs (Schmertmann and Palacios, 1979). The arrival of the return wave to the top of the drill rods causes the rods to pull away from the hammer and effectively stops further transfer of energy from hammer to rods. The longer the drill rods, the longer is the hammer-rod contact time and the more hammer energy that enters the rods. It is this transferred energy in the drill rods that is doing the work in the SPT sampler penetration.

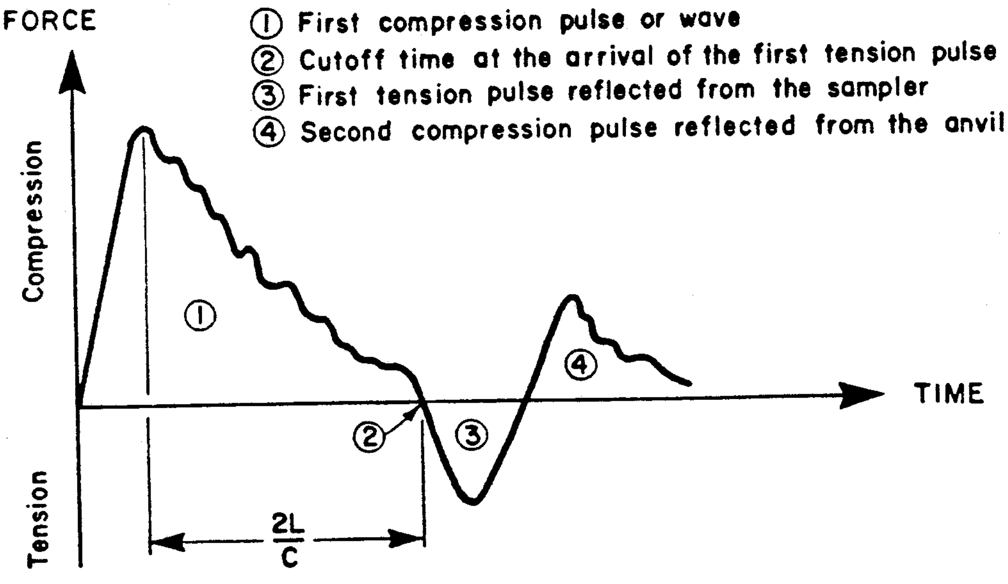

Figure 1. Idealized Force-Time Waveform Recorded by Load Cell in SPT Drill Rods

For impact wave propagation in one direction in a uniform unsupported elastic rod, the force (F) at a point in the rod is equal to the particle velocity (v) at that point times the impedance (Z), i.e. F=Zv. The impedance is a material constant defined as EA/c, where E is the Young's modulus of the rod, A is the cross-sectional area of the rod and c is the velocity of wave propagation in the rod. Consequently, in an elastic rod of uniform cross-section, the particle velocity is proportional to the force at a point, as long as there are no wave reflections from external forces acting on the rod. This proportionality relationship is the basis for evaluating the soil resistance from stress wave measurements in piles (Hussein and Goble, 1987).

The SPT, however, is a more complex dynamic system. From the point of hammer impact on the anvil in a typical safety hammer system, the stress wave travels through a hammer guide rod, drill rods, sampler and couplings or adaptors connecting the different parts, all of which can have different cross-sectional areas or impedances. When a stress wave encounters a sudden change in cross-sectional area, part of the wave is reflected back from the interface and part is transmitted. The sign of the reflected wave depends on the sign of the initial wave and whether or not the area is increased or decreased. Thus the different impedances in the SPT drill rod system cause various wave reflections in the system. The hammer/anvil geometries and soil resistances also affect the stress wave propagating in the drill rods. Therefore, the theoretical force-velocity proportionality relationship does not hold, and both force and velocity measurements are needed to fully characterize the stress waves in the SPT system.

Independent force and velocity measurements in the drill rods will also allow a more fundamental approach to determining the energy transfer in the drill rods due to hammer impact (Sy and Campanella, 1991). The transferred energy can be calculated by time integration of the force times velocity data.

FIELD WORK

The field work was conducted at the University of British Columbia (UBC) in-situ testing research site in McDonald's Farm, an abandoned farm on Sea Island, the site of the Vancouver International Airport south of Vancouver, British Columbia, Canada. Sea Island is located in the Fraser River delta and is contained by a system of dykes to prevent flooding. The site is approximately level. The mean groundwater table at the site is about 5 ft (1.5 m) below ground surface and varies with the tidal fluctuations of the adjacent Fraser River.

The soil conditions at McDonald's Farm consist of 7 ft (2 m) of soft organic clayey silt overlying an 8 ft (2.5 m) thick zone of silty fine sand underlain by about 36 ft (11 m) of medium to coarse sand. The sand stratum is variable in density with occasional seams of silt. Underlying the sand is a deep deposit of normally consolidated silty clay which extends to a depth of about 350 ft (105 m) above very dense glacial deposits. Figure 2 shows piezometer cone penetration test (CPT) data and soil profile at the site. Full details of the research test site are given in Campanella et al. (1983).

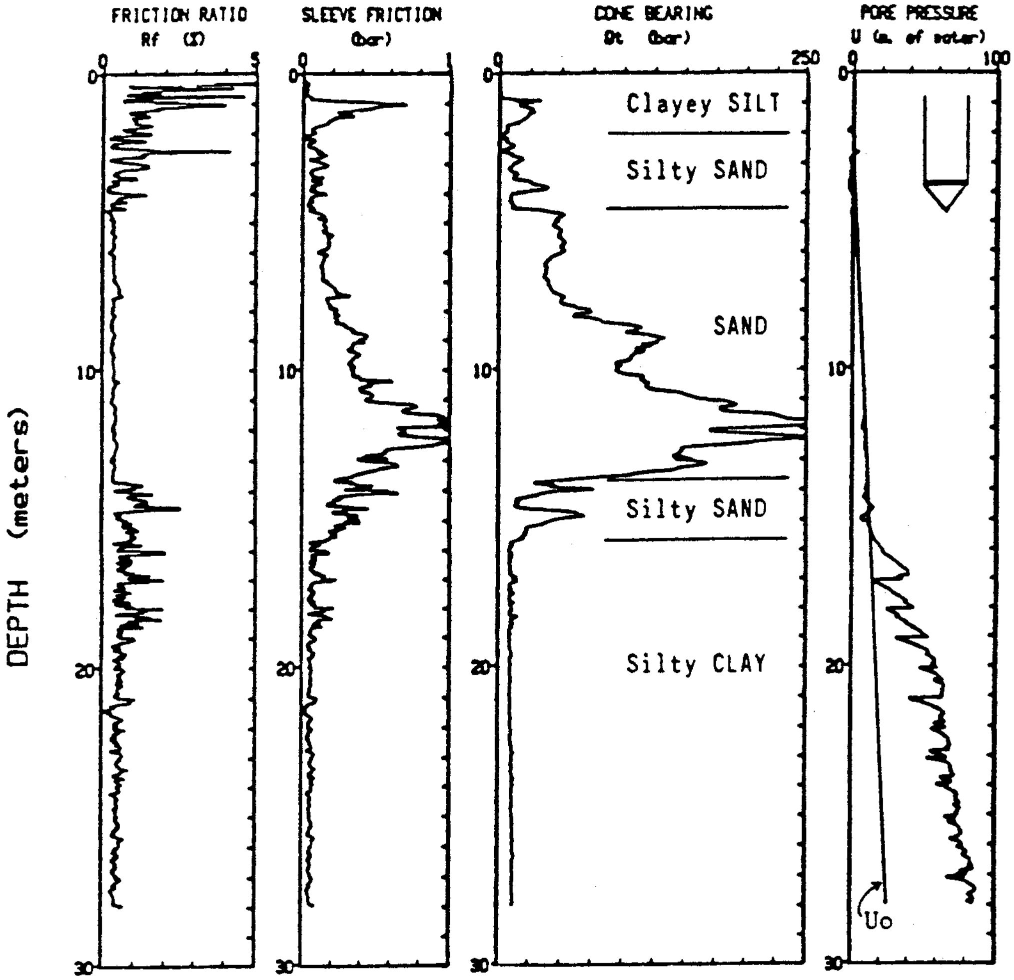

Figure 2. Cone Penetration Test Profile

The SPT's were conducted between 5 ft (1.5 m) and 30 ft (9.1 m) depths in a mud rotary drill hole using a Gardner Denver 1000 drill rig. The SPT was performed in accordance with ASTM D 1586-84 using a safety hammer with two turns of rope around the cathead. Figure 3 shows dimensions of the safety hammer used. A modified Binary Instruments Inc. SPT calibrator (Hall, 1982) was used to measure the force-time histories of the impact waves in the drill rods with a load cell. In addition to the force transducer, an accelerometer was attached adjacent to the load cell to record accelerations in the rods. Both instruments are piezoelectric type transducers which are robust, stable and have fast dynamic response. The transducers were attached 5.8 ft (1.8 m) below the anvil location. The force and acceleration measurements of the SPT blows were recorded on a Nicolet 4094 digital oscilloscope with a 15 bit A/D resolution. For both channels, data samples were obtained at a time interval of 0.01 ms.

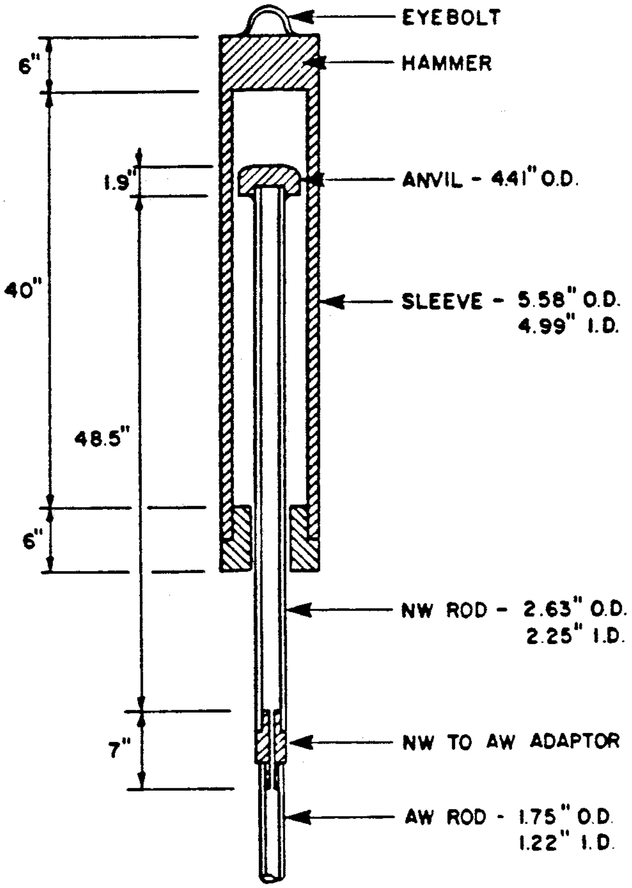

Figure 3. Safety Hammer Used in this Study [1 inch=25.4 mm]

MEASURED STRESS WAVES

Stress wave measurements of two typical SPT blows, one at 5 ft (1.5 m) depth in the soft silt and another at 30 ft (9.1 m) depth in the medium to dense, fine to medium grained sand, are presented below.

Figure 4 shows the stress wave measurements for the first blow of the SPT at 5 ft (1.5 m) depth where the recorded N value was 2. The SPT sampler penetrated 8 inches (200 mm) during this blow. The top two plots are the recorded force and acceleration time histories. The sign convention used is positive force for compression wave and negative force for tension wave, and positive acceleration or velocity for downward motion and negative acceleration or velocity for upward motion. The measured peak compression force is 19 kips (85 kN) and the maximum acceleration is over 2500 g. Figure 4 also shows the velocity trace obtained by integration of the recorded acceleration wave trace. The peak velocity of the primary compression pulse is 11 ft/sec (3.4 m/s). The maximum velocity reached 15 ft/sec (4.6 m/s) when the initial compression pulse reflected back from the sampler tip as a large tension wave because of the very small soil resistance acting on the sampler. At the end of the 20 ms record, the drill rods were still

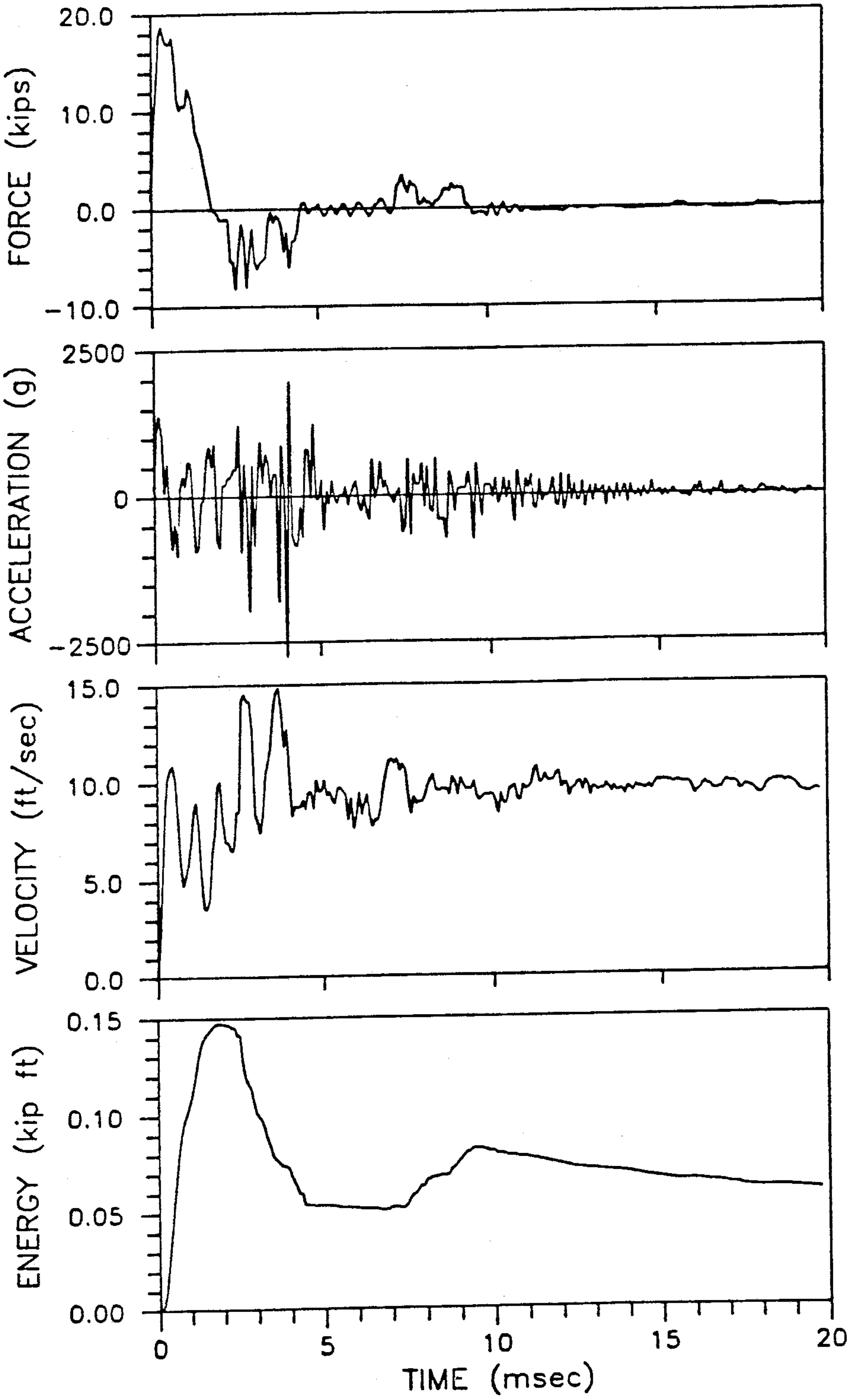

Figure 4. Measured Force, Acceleration, Velocity and Energy Traces for SPT Blow 1 at 5 ft Depth [1 ft= 0.3 m; 1 kip=4.4 kN; 1 ft/sec=0.3 m/s; 1 kip ft=1.4 kJ]

moving down at a velocity of about 10 ft/sec (3.0 m/s). Integration of this velocity trace yields a calculated displacement of only 2.5 inches (64 mm) at 20 ms. Obviously the record length of 20 ms was not long enough to capture the complete event for this blow. Finally, the bottom plot in Figure 4 shows the calculated energy from time integration of force times velocity. For this blow, the maximum energy transfer (ENTHRU) is 0.15 kip-ft (203 J), which is 42 % of the theoretical free fall hammer energy of 0.35 kip-ft (475 J). Note that this maximum energy occurs at 1.85 ms when the tensile reflection from the sampler bottom reaches the transducer location in the drill rods.

The same blow above is replotted in Figure 5A showing the force (F) and velocity times impedance (VEA/c) wave traces. To calculate the impedance, the cross-sectional area of the AW rod, rather than that of the larger NW rod or the load cell, was arbitrarily selected. This type of proportional stress wave plot is more illuminating and it illustrates several key features. First of all, if force and velocity are proportional within the first compression pulse as would be expected for wave propagation in a uniform rod with only tip resistance, they will plot on top of each other. Figure 5A shows that proportionality does not exist at the two velocity peaks in the primary compression pulse. The first velocity peak at 0.45 ms is due to the hammer impact, and the effect of the hammer/anvil geometries is shown by the separation of the force and velocity peaks in this region. The second velocity peak at 1.2 ms is caused by the reflection of the primary pulse from the load cell up to the top of the drill rods (or anvil) and back. Note that the cross-sectional area of the load cell is about twice that of the NW or AW rods. The reflection here again results in the separation of the force and velocity traces. The third velocity peak at 1.85 ms is the tensile reflection of the impact compression wave from the sampler. As expected, the tension force cutoff also occurs at this time. Reflection of the return tension wave from the top of the rods is indicated by the fourth velocity peak and the fifth velocity peak corresponds to the second cycle return wave from the sampler.

Figure 5A also shows that the point of impact is much better defined by the sharper initial velocity peak than by the initial force peak. The time interval between the first velocity peak (impact) and the third velocity peak (return wave), or the tension cutoff point, is 1.4 ms. This time corresponds to the theoretical 2L/c time for the wave to travel from the load cell to the sampler tip, where L=12.2 ft (3.7 m), and back to the load cell. Note that the 2L/c is not measured from the beginning of the force time pulse to the tension cutoff point, as is commonly assumed (e.g. ASTM D 4633-86).

Figure 6 shows the measured force, acceleration, velocity and energy time histories for the 28th blow at 30 ft (9.1 m) depth in which the recorded N value was 21. The visually observed sampler penetration for this blow is 0.5 inch (13 mm). The recorded peak force is 20 kips (89 kN) and the maximum acceleration is 2000 g. The peak velocity at impact is 11 ft/sec (3.4 m/s), and the velocity is practically zero at the end of the 20 ms record. The maximum energy at the transducer location is 0.21 kip-ft (285 J) or 60 % of the theoretical free fall hammer energy.

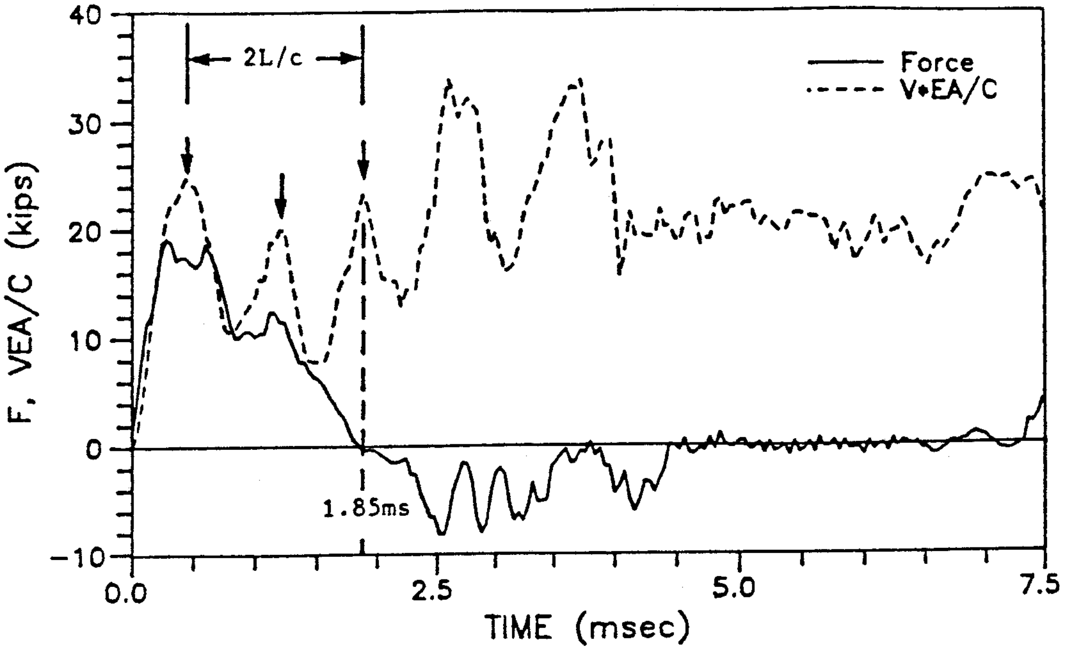

Figure 5A. Measured Force and Velocity Traces for SPT Blow 1 at 5 ft Depth [1 ft=0.3 m; 1 kip=4.4 kN]

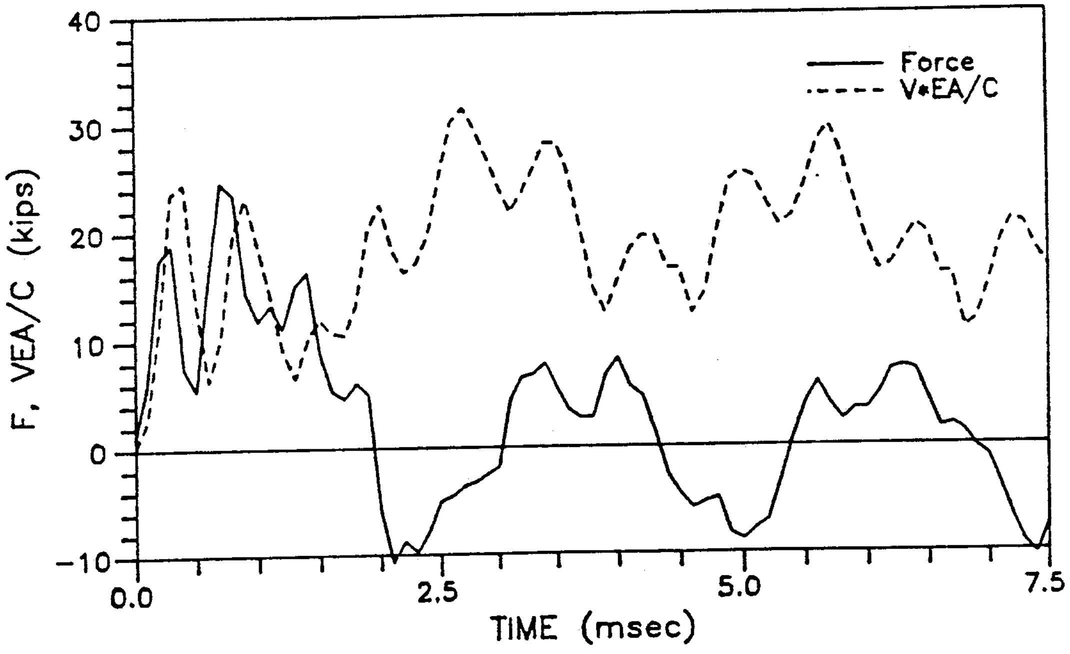

Figure 5B. Computed Force and Velocity Traces for SPT Blow 1 at 5 ft Depth [1 ft=0.3 m; 1 kip=4.4 kN]

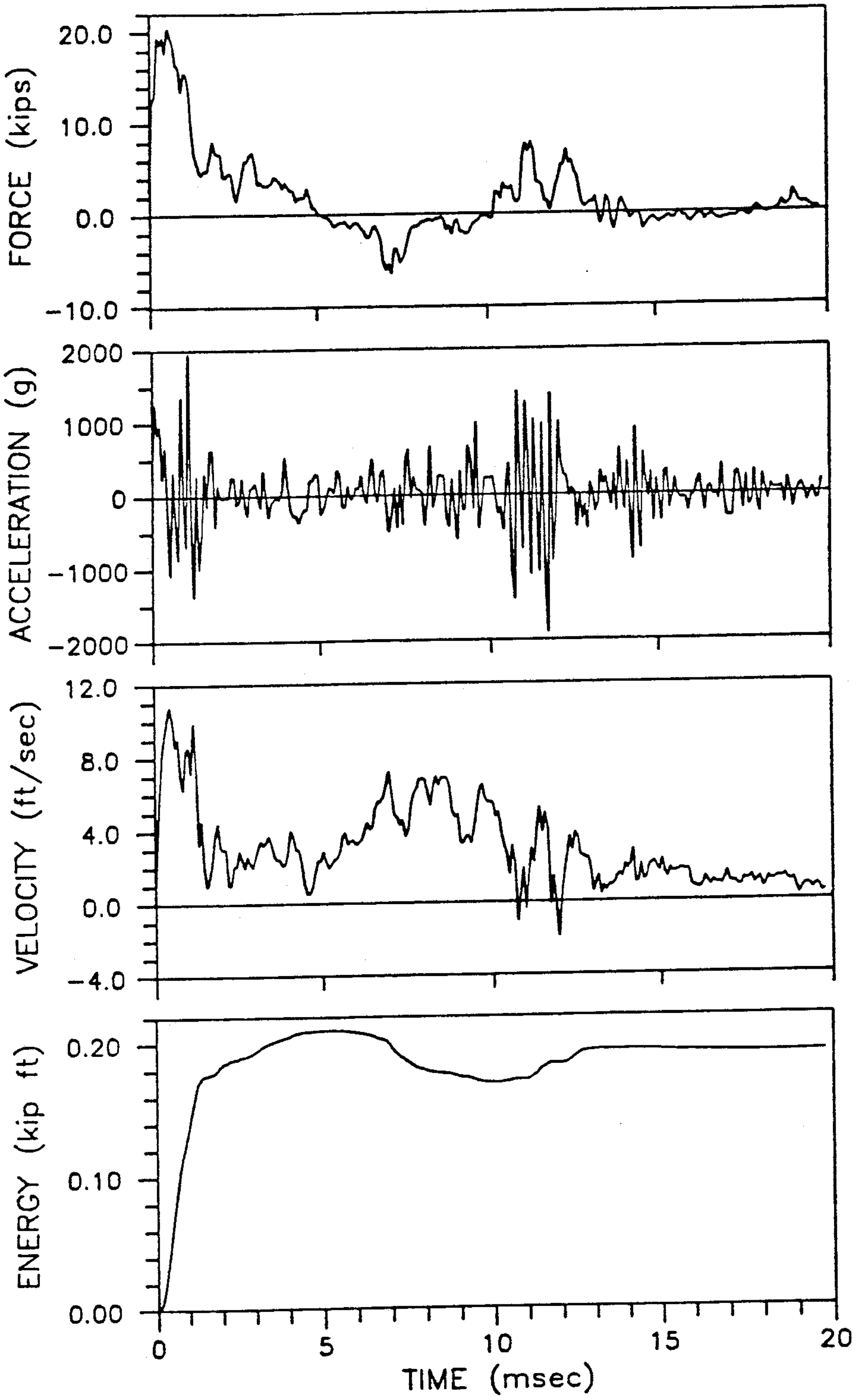

Figure 6. Measured Force, Acceleration, Velocity and Energy Traces for SPT Blow 28 at 30 ft Depth [1 ft= 0.3 m; 1 kip=4.4 kN; 1 ft/sec=0.3 m/s; 1 kip ft=1.4 kJ]

Figure 7A shows the F and VEA/c traces for the same blow presented in Figure 6. The force and velocity traces are again not proportional within the first compression pulse due to the reflections from the different impedances in the SPT rod system. The tensile reflection of the first compression pulse from the sampler occurs at 5.0 ms. Note the reflected velocity peak at this time is much smaller, indicating the larger soil resistance encountered at the sampler. The time interval from the first impact velocity peak to the first return velocity peak, or the tension cutoff, is 4.5 ms, which again corresponds to the theoretical 2L/c in which L=37.2 ft (11.3 m) for this test. Within the first compression and the first tension wave pulses, there are velocity peaks appearing regularly at about 0.7 ms interval. This interval is the time it takes for the wave to travel from the load cell to the top of the rods (anvil) and back. These reflections are caused primarily by the presence of the load cell in the SPT rod system.

WAVE EQUATION ANALYSIS

The wave equation analysis of the SPT was performed using the GRLWEAP program written by Goble Rausche Likins and Associates, Inc. (1990) and based on the Smith (1960) one-dimensional wave equation model for pile driving analysis. In the Smith wave equation model, the driving system (i.e. the hammer and anvil in this SPT study) and pile (or drill rods) are represented by a series of masses and springs. The soil is represented by a series of elastic-plastic springs and linear dashpots. The two SPT blows discussed above, Blow 1 at 5 ft (1.5 m) depth and Blow 28 at 30 ft (9.1 m) depth, were analyzed. The objective of the analysis was to evaluate the wave equation model for prediction of the SPT sampler penetration and the force and velocity waveforms in the drill rods.

In the analysis, the safety hammer was modelled as a 52 inch (1.3 m) thick element. The anvil was modelled as a "helmet" mass and a "hammer cushion" spring. The hammer guide rod, drill rods, load cell, sampler and couplings or adaptors were also modelled as discrete elements with appropriate weights, lengths and cross-sectional areas. Because of the units and dimensions embedded in the GRLWEAP program, rod elements smaller than 0.5 ft (0.15 m) are not practical due to the very small numbers involved and the possibility of roundoff errors in the computations. Consequently, a minimum element size of 0.5 ft (0.15 m) was used. This placed some limitations in accurately modelling the adaptors, couplings and load cell, and consequently, average areas over reasonable segment lengths were used for these elements.

For consistency, the same hammer-anvil-drill rod model parameters were used for the two SPT blows analyzed, except for the difference in the drill rod length. A very small hammer damping was assigned in the analysis and a nominal rod damping as recommended in the GRLWEAP manual for steel pile was used.

For the soil model, conventional Smith damping coefficients and quake values as recommended in the GRLWEAP manual were selected. The static soil resistance acting on the sampler is another input parameter in the wave equation analysis. The soil resistances acting on the sampler tip and sides were estimated from CPT tip resistance and sleeve

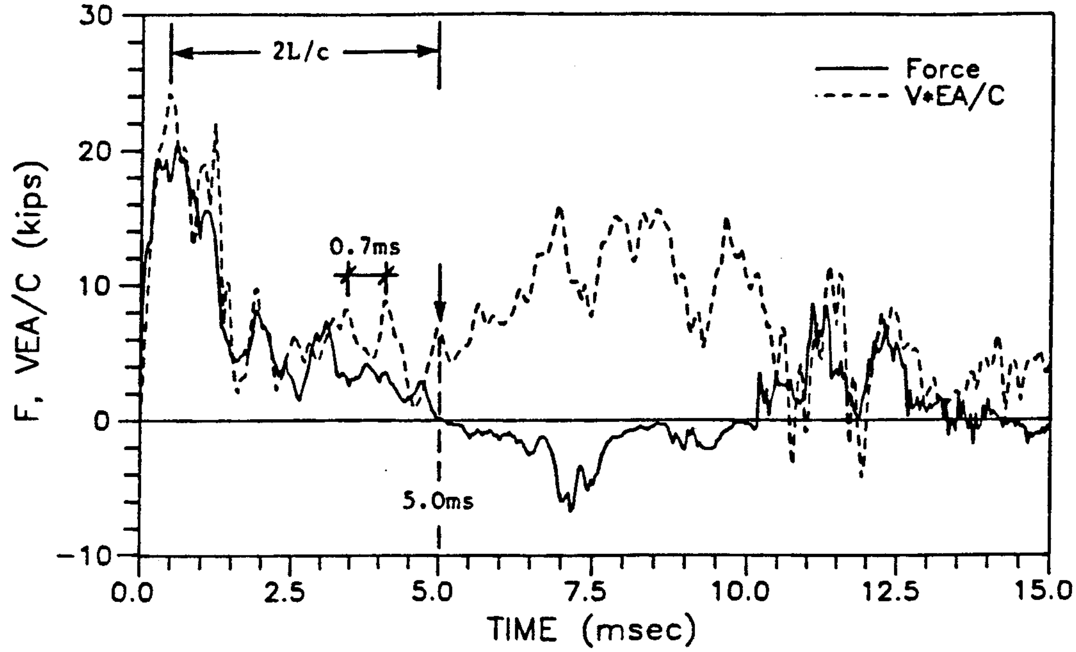

Figure 7A. Measured Force and Velocity Traces for SPT Blow 28 at 30 ft Depth [1 ft=0.3 m; 1 kip=4.4 kN]

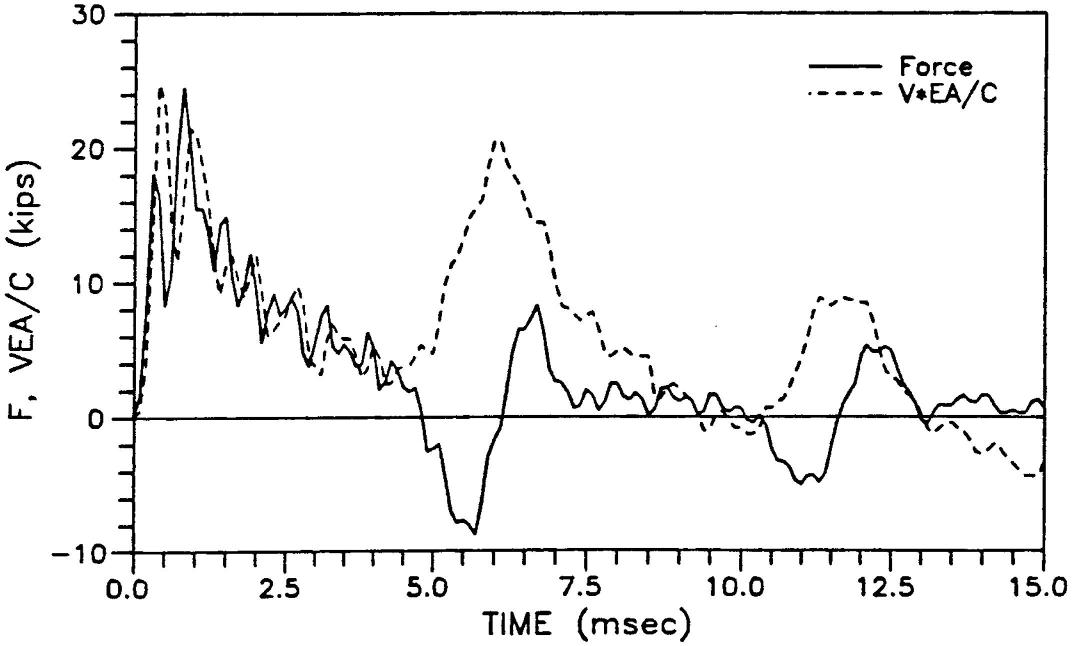

Figure 7B. Computed Force and Velocity Traces for SPT Blow 28 at 30 ft Depth [1 ft=0.3 m; 1 kip=4.4 kN] friction data following the procedure proposed by Schmertmann (1979). The estimated total resistances are 0.2 kips (0.9 kN) with a sampler embedment of 8 inches (200 mm) for the SPT blow at 5 ft (1.5 m), and 2.75 kips (12.2 kN) with a sampler embedment of 18 inches (445 mm) for the SPT at 30 ft (9.1 m).

The wave equation analysis also requires the input of hammer efficiency which is used to calculate an initial impact velocity to start off the finite difference computation. Hammer efficiency values were selected so that the computed energy values at the transducer location (ENTHRU) are similar to those measured in the field. Consequently, hammer efficiencies of 60 % for the blow at 5 ft (1.5 m) and 70 % for the blow at 30 ft (9.1 m) were needed to match the measured energies in the drill rods. These values are within the range commonly measured for safety hammers (Kovacs and Salomone, 1982; Robertson et al. 1983).

The GRLWEAP program typically outputs the predicted blow count, maximum and minimum stresses in the rods, and the ENTHRU at the top of the rods, for each input soil resistance value. It also summarizes, for every element or segment in the SPT rod system, the maximum and minimum forces and stresses, the maximum velocity, displacement and maximum energy transfer. In addition, a complete output of force, stress, acceleration, velocity, and displacement versus time for every element can be obtained.

A parametric study was conducted to investigate the influence of various parameters including hammer length, hammer, rod and soil damping values, drill rod couplings, slack at rod joints, analysis time step, rod element size and soil resistances. It was found that the most significant input parameters affecting the computed waveforms are the impedances of the system above the load cell level, including the hammer itself, and the damping values for the hammer, rod and soil elements. These factors, however, do not significantly affect the calculated blow count or sampler penetration (inch/blow), and the ENTHRU values. These latter results are more sensitive to the input soil resistance and hammer efficiency values. This latter conclusion was also found in studies by previous investigators (e.g. McLean et al. 1975).

Figure 5B shows the computed F and VEA/c traces for Blow 1 at 5 ft (1.5 m) depth. Overall, the computed traces map out the trend of the measured waveforms in Figure 5A. The computed impact force and velocity values at 0.3 ms are also similar to the measured values. In the first compression pulse, however, there is an additional third small spike in the computed traces that are not evident in the field data. The tension cutoff time occurs at 1.85 ms in both traces. The computed velocity profile, after arrival of the tensile reflected wave from the sampler, shows the same large peaks as in the measured waveform. The measured force trace beyond 2 ms and the velocity trace beyond 4 ms are much more damped than the corresponding computed traces. Introducing slack at rod joints or increasing the hammer, rod or soil damping values in the wave equation analysis would improve the match in this portion of the waveform. However, these refinements could not be consistently applied to the other blows analyzed and are, therefore, not shown here.

With an input hammer efficiency of 60 %, the computed ENTHRU at the transducer location for the 5 ft (1.5 m) SPT analysis is 0.15 k-ft (203 J). The computed sampler penetration, or inverse of the blow count, is 5 inches (130 mm), compared to the field observed value of 8 inches (200 mm). This suggests that the ultimate soil resistance acting on the sampler in the field was less than the 0.2 kips (0.9 kN) estimated from CPT data. This is not surprising since the first blow in a SPT is often in soils previously disturbed by the drilling.

Figure 7B shows the computed F and VEA/c traces for Blow 28 at 30 ft (9.1 m) depth. Again overall, the computed traces follow the general trend of the measured waveforms in Figure 7A, although the computed profiles display sharper oscillations. Increasing the hammer or pile damping in the wave equation model would damp out these oscillations, improving the force match but not the velocity. Again, these refinements were not considered consistent. Within the first compression pulse, the computed velocity trace has about the same number and frequency of peaks as in the measured trace. The computed tension cutoff at 4.7 ms is close to the measured value at 5.0 ms. For an input hammer efficiency of 70 %, the calculated ENTHRU at the transducer location is 0.21 k-ft (285 J). The calculated penetration of 0.5 inch (13 mm) is similar to the field observed value for this blow.

In summary, the one-dimensional wave equation model of the SPT predicts the ENTHRU and blow count or sampler penetration well, provided appropriate soil resistance and hammer efficiency values are input. The limited study conducted for the safety hammer indicates that the main features in the measured stress waves can be reasonably simulated in the computer analysis using small segment lengths and appropriate cross-sectional areas to model the drill rod and sampler system, and using conventional soil parameters.

CONCLUSIONS

The SPT is a complex dynamic system. The recorded force and integral of measured acceleration (or particle velocity) traces from the SPT are complicated and show wave reflections from the different impedances in the drill rod and sampler system. It is shown that both force and motion measurements are needed to fully characterize the stress wave propagation in the SPT system. A study of the force and velocity traces can give considerable insight into the dynamics of the SPT, as well as allowing a more fundamental approach of calculating the impact energy entering the drill rods. The impact velocity peak is often sharper than the force peak and allows a more accurate determination of the wave return time (2L/c). The 2L/c time can be determined from the time interval between the first velocity peak and the return velocity peak or the tension force cutoff point. It is shown that the one-dimensional wave equation model can adequately model the SPT for prediction of ENTHRU and sampler penetration. The wave equation model also has the potential for simulating the stress waves in the SPT system.

ACKNOWLEDGEMENTS

The authors wish to acknowledge the financial support of the NSERC Strategic Grant for this study. The first author also wishes to acknowledge the STARS scholarship provided by the Science Council of B.C. in cooperation with Klohn Leonoff Ltd. The support and interest of Foundex Explorations Ltd., B.C. Ministry of Transportation and Highways, and B.C. Hydro are appreciated. The valuable assistance of Wang J.W. and E. Naesgaard, and especially Scott Jackson, UBC Civil Eng. senior electronics technologist, is much appreciated.

REFERENCES

1. J Adam, discussion of The Standard Penetration Test by VFB deMello, Proc. 4th PanAm. Conf. on Soil Mech. and Found. Engin., Vol.3, June 1971, 82-84.
2. ASTM D 1586-84, Standard Method for Penetration Test and Split-Barrel Sampling of Soils.
3. ASTM D 4633-86, Standard Test Method for Stress Wave Energy Measurement for Dynamic Penetrometer Testing Systems.
4. PJ Bosscher & DR Showers, Effect of Soil Type on Standard Penetration Test Input Energy, ASCE, J.Geot.Eng., Vol.113, No.4, April 1987, 385-389.
5. RG Campanella, PK Robertson & D Gillespie, Cone Penetration Testing in Deltaic Soils, Can.Geot.J., Vol.20, No.1, Feb.1983, 23-35.
6. RA Ellstein, Dynamic Cone, Wave Equation and Microcomputers: The Mexican Experience, Penetration Testing 1988, ISOPT-1, Ed DeRuiter, 1988, 341-345.
7. AJ Gallet, Use of the Wave Equation to Investigate Standard Penetration Test Field Measurements, MEng Thesis, University of Florida, Gainesville, 1976.
8. Goble Rausche Likins and Associates, Inc., GRLWEAP Program, Wave Equation Analysis of Pile Driving, 1990.
9. JR Hall, Drill Rod Energy as a Basis for Correlation of SPT Data, Proc. ESOPT-2, Amsterdam, 1982, 57-60.
10. CS Hanskat, Wave Equation Simulation of the Standard Penetration Test, MEng Thesis, University of Florida, Gainesville, 1978.
11. M Hussein & GG Goble, Qualitative Evaluation of Force and Velocity Measurements during Pile Driving, Dyn.Response of Pile Foundations, ASCE Geot.Spec.Publ. No.11, 1987, 166-183.
12. WD Kovacs & LA Salomone, SPT Hammer Energy Measurement, ASCE, J.Geot.Eng., Vol.108, No.GT4, April 1982, 599-620.
13. FG McLean, AG Franklin & TK Dahlstrand, Influence of Mechanical Variables on the SPT, Proc. of the Conf. on In Situ Meas. of Soil Properties, ASCE, Vol.1, June 1975, 287-318.
14. A Palacios, The Theory and Measurement of Energy Transfer during Standard Penetration Test Sampling, PhD Thesis, University of Florida, Gainesville, 1977.
15. CO Riggs, GM Mathes & CL Rassieur, A Field Study of an Automatic SPT Hammer System, Geot.Testing J.,Vol.7, No.3, Sep.1984, 158-163.

16. PK Robertson, RG Campanella & A Wightman, SPT-CPT Correlations, ASCE, J.Geot.Eng., Vol.109, No.11, Nov.1983, 1449-1459.
17. JH Schmertmann, Use the SPT to Measure Dynamic Soil Properties?- Yes, But..!, Dynamic Geot.Testing, ASTM STP 654, 1978, 341-355.
18. JH Schmertmann, Statics of SPT, ASCE, J.Geot.Eng.Div., Vol.105, No.GT5, May 1979, 655-670.
19. JH Schmertmann & A Palacios, Energy Dynamics of SPT, ASCE, J.Geot.Eng.Div., Vol.105, No.GT8, Aug.1979, 909-926.
20. EAL Smith, Pile Driving Analysis by the Wave Equation, ASCE, J.Soil Mech.&Found.Div., Vol.86, No.SM4, 1960, 35-61.
21. TV Smith, A Summary of Energy Calibration Tests on SPT Equipment, MEng Thesis, University of Florida, Gainesville, 1977.
22. A Sy & RG Campanella, An Alternative Method of Measuring SPT Energy, 2nd Int.Conf.on Recent Advances in Geot.Earthquake Eng.& Soil Dynamics, St. Louis, Missouri, Mar.1991.